Supporting Information

Electrospun ZIF Derived cavity porous carbon nanofibers as freestanding cathode for lithium-oxygen batteries with ultralow overpotential

School of Energy and Environmental Engineering, University of Science and Technology Beijing, Beijing 100083, China; Beijing Key Laboratory of Resource-oriented Treatment of Industrial pollutants, Beijing 100083, China

Corresponding author: congjuli@126.com

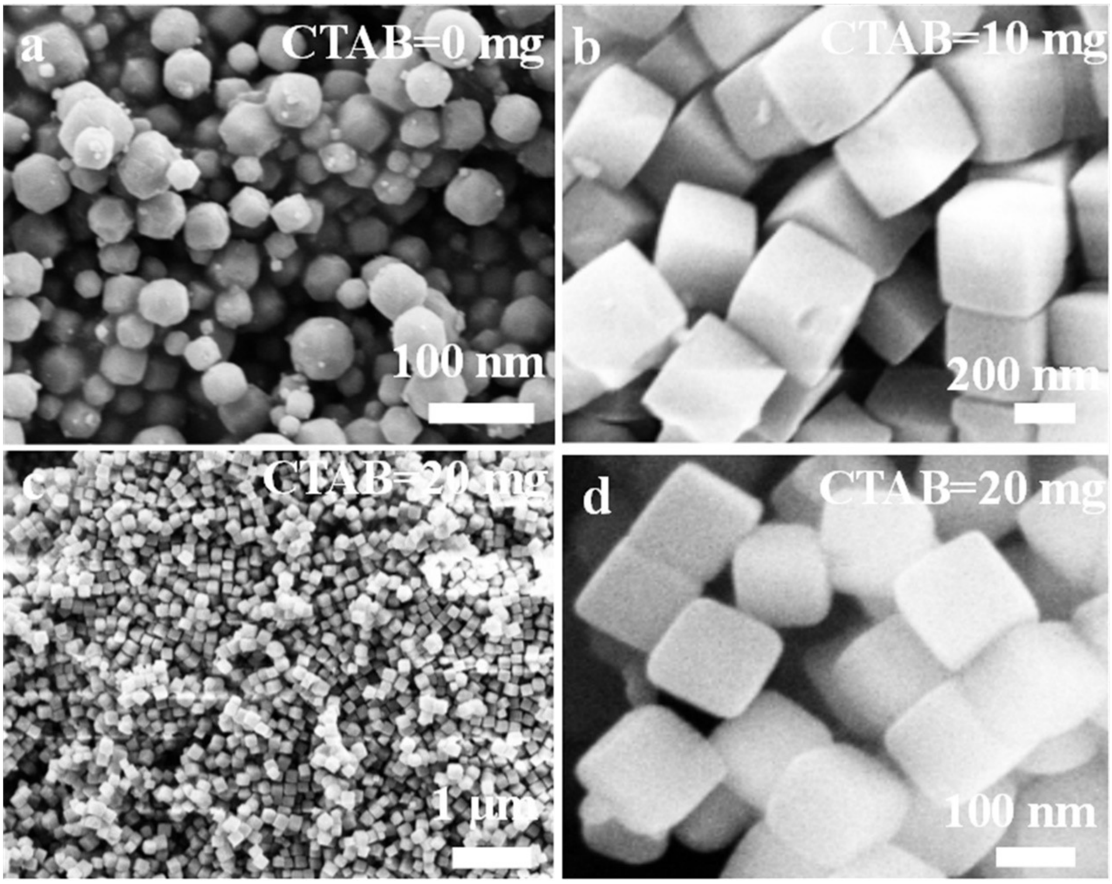

Fig. S1. SEM images of (a, b) pure ZIF-8 and cubic ZIF-8 prepared with CTAB contents of 0, 10 mg and (c-d) pure cubic ZIF-8 prepared with CTAB contents of 20 mg at different magnifications.

The average sizes are determined as 380 and 150 nm for the cubic ZIF-8 when the added CTAB amounts are 10 and 20 mg, respectively. The more CTAB added, the faster the nucleation speed and the smaller the size.

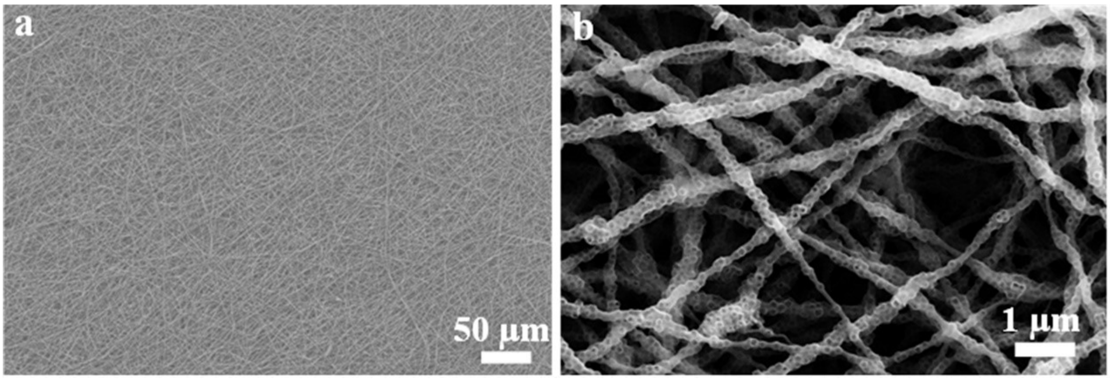

Fig. S2. FE-SEM images of Zn/CoNC@CPCFs, respectively (different magnification).

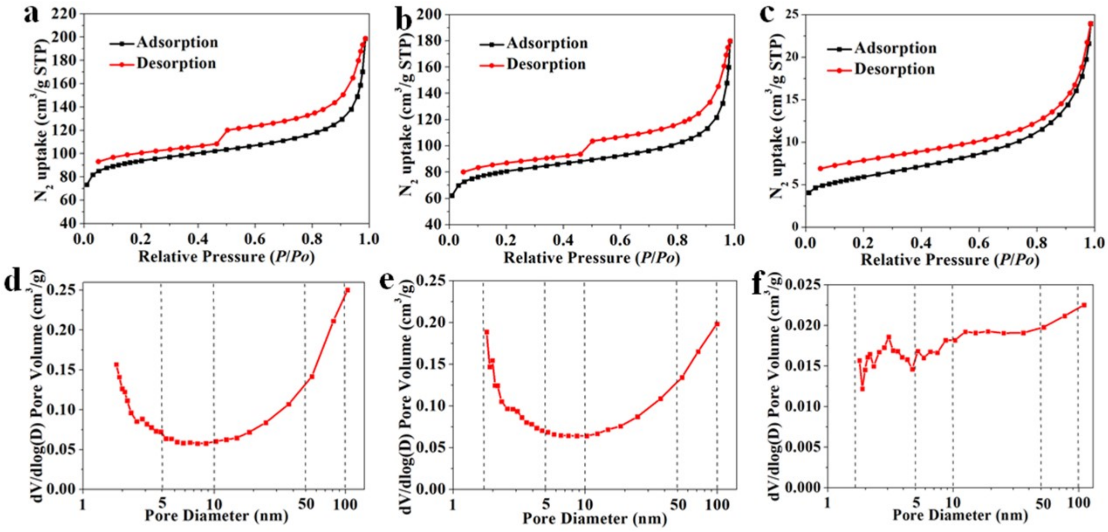

Fig. S3. Nitrogen adsorption isotherms and pore size distribution curves of Zn/CoNC@CPCFs (a, d), ZnNC@CPCFs (b, e) and CoNC@ CFs (c, f).

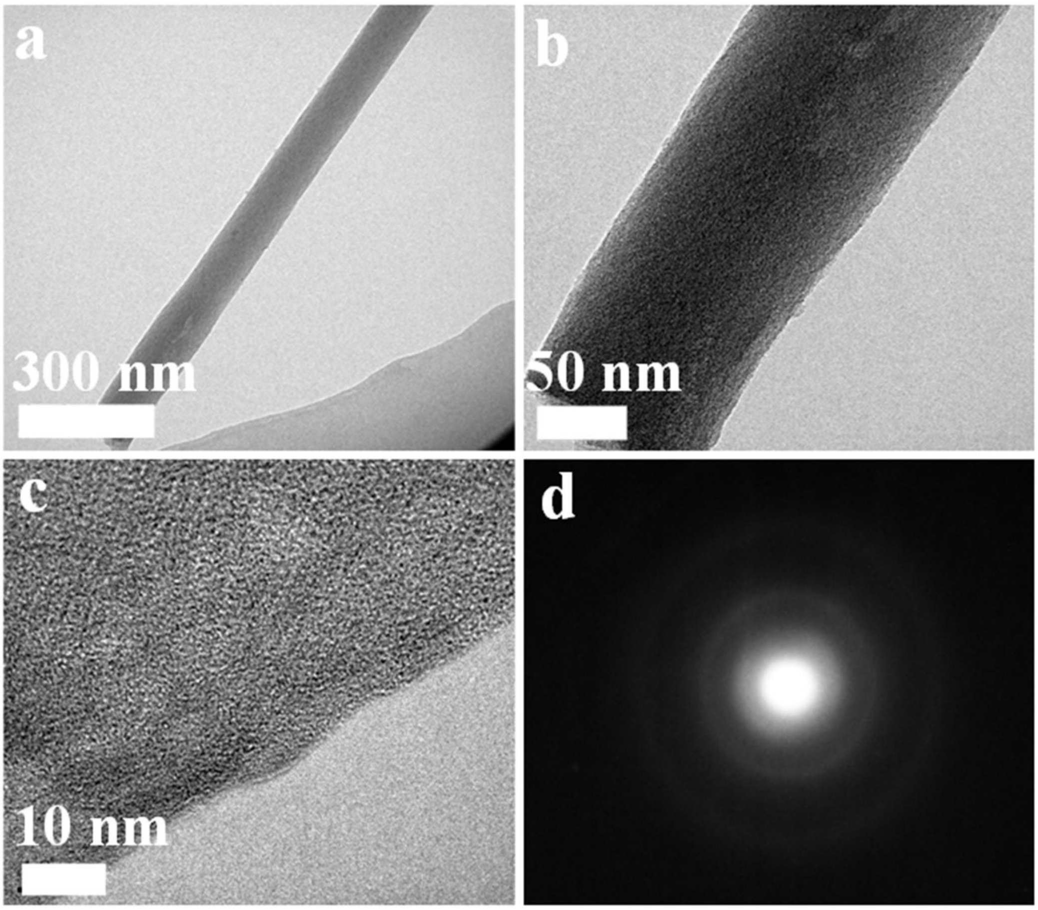

Fig. S4. TEM image (a-c) and HRTEM image (d, inset of corresponding SAED pattern) of CoNC@ CFs.

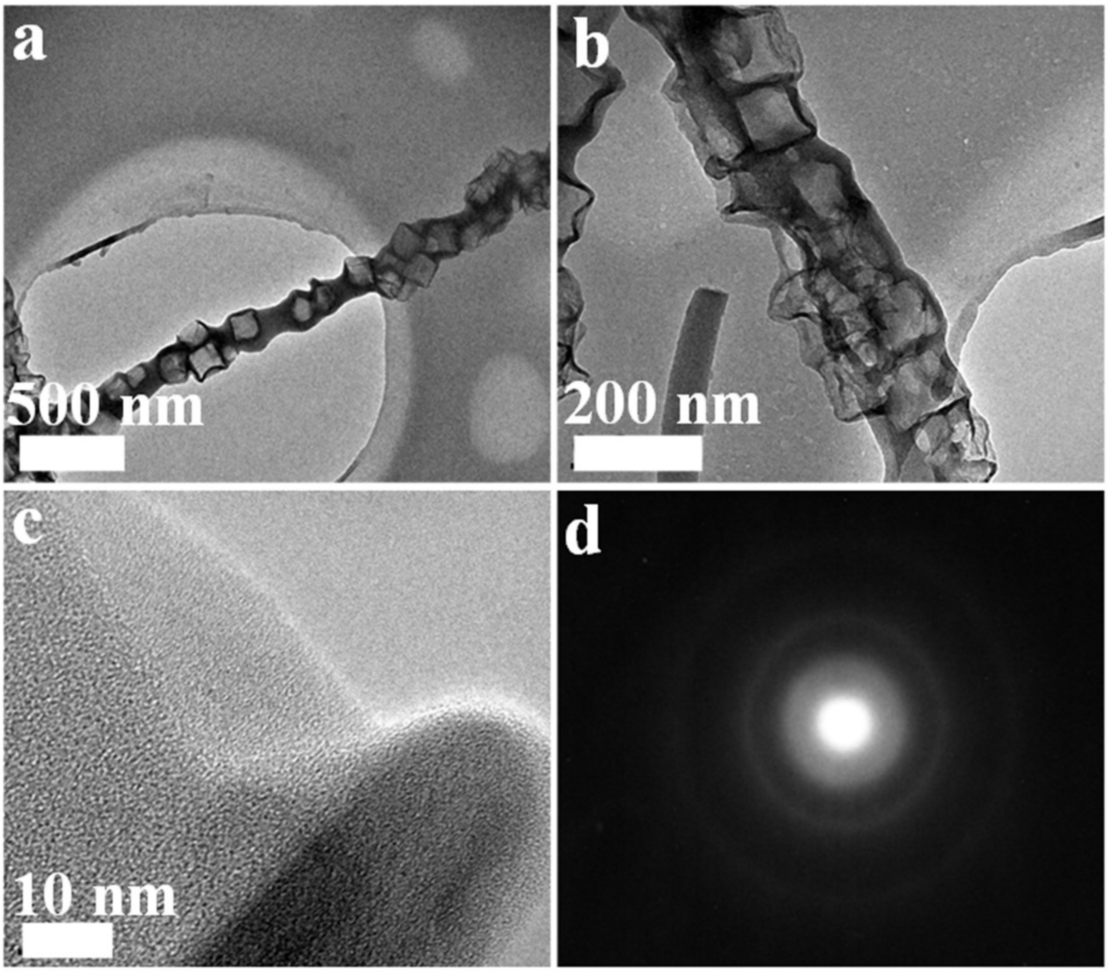

Fig. S5. TEM image (a-c) and HRTEM image (d, inset of corresponding SAED pattern) of ZnNC@CPCFs.

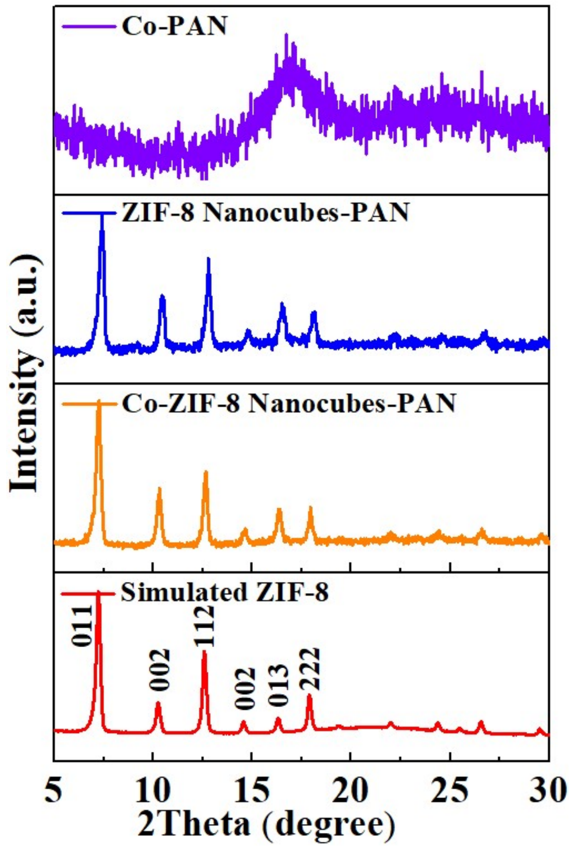

Fig. S6. XRD patterns of as-prepared three samples.

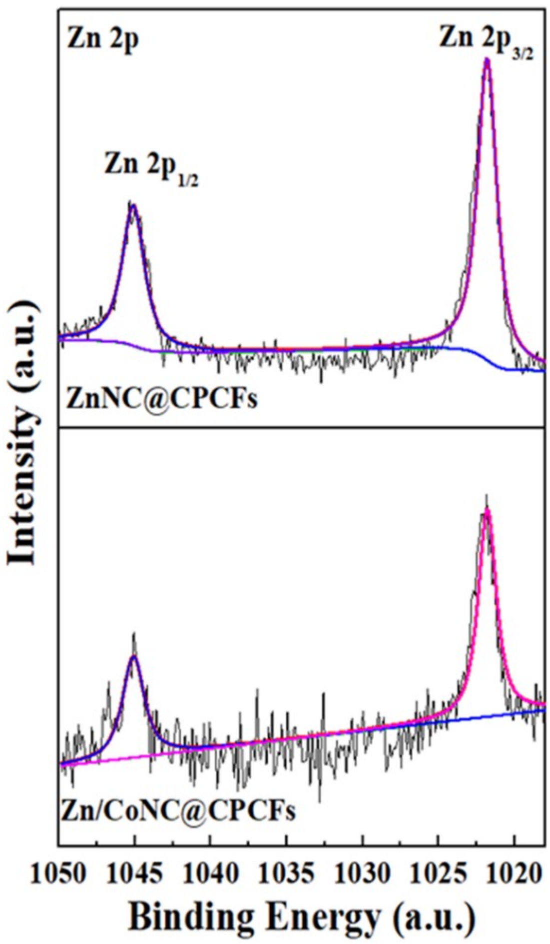

Fig. S7. The X-ray photoelectron spectroscopy (XPS) measurement.

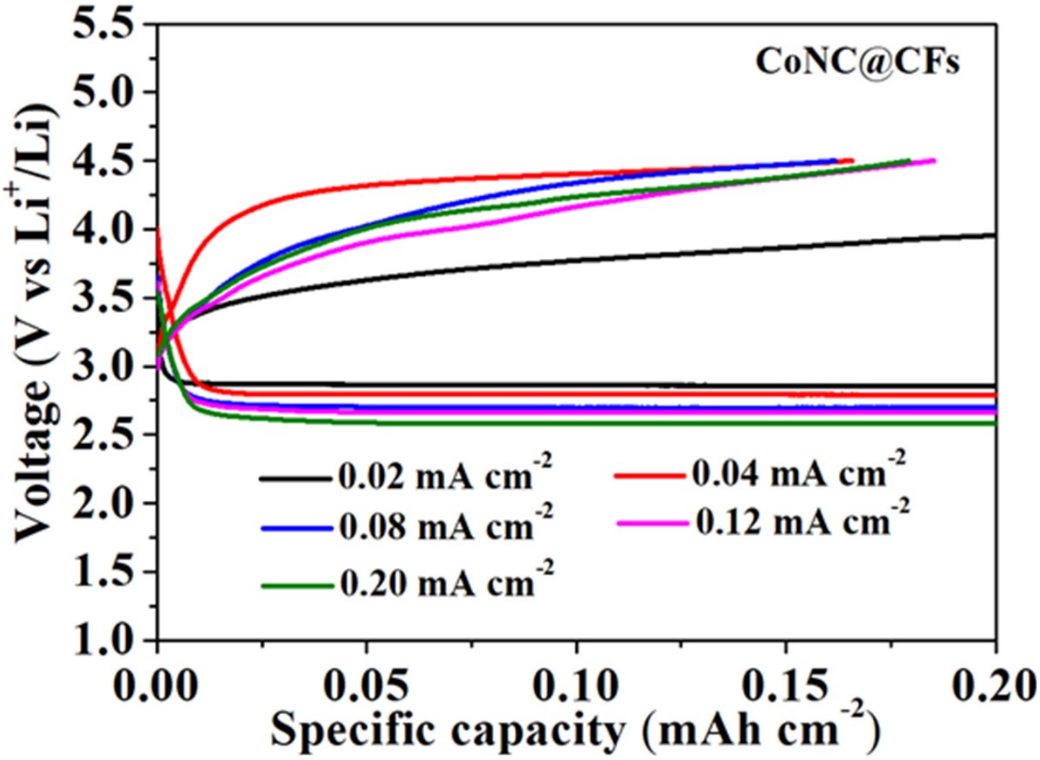

Fig. S8. Discharge–charge voltage curves of CoNC@CFs electrodes at different current densities with a cut-off capacity of 0.20 mAh cm^{-2}.

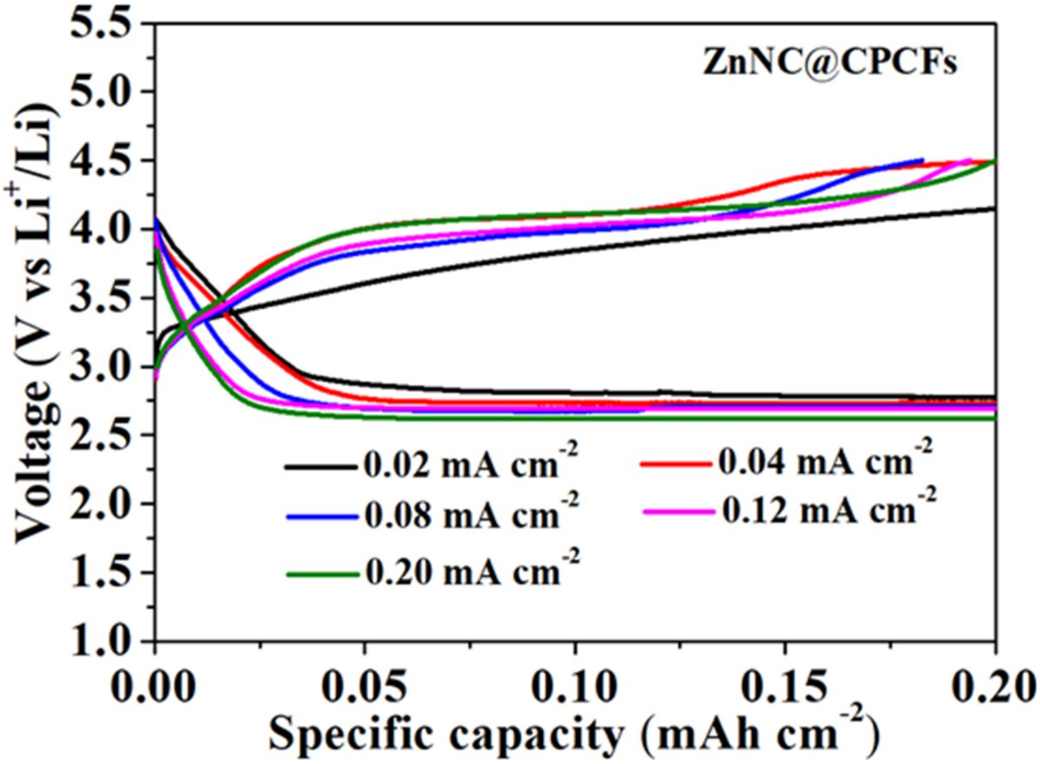

Fig. S9. Discharge–charge voltage curves of ZnNC@CPCNFs electrodes at different current densities with a cut-off capacity of 0.20 mAh cm^{-2}.

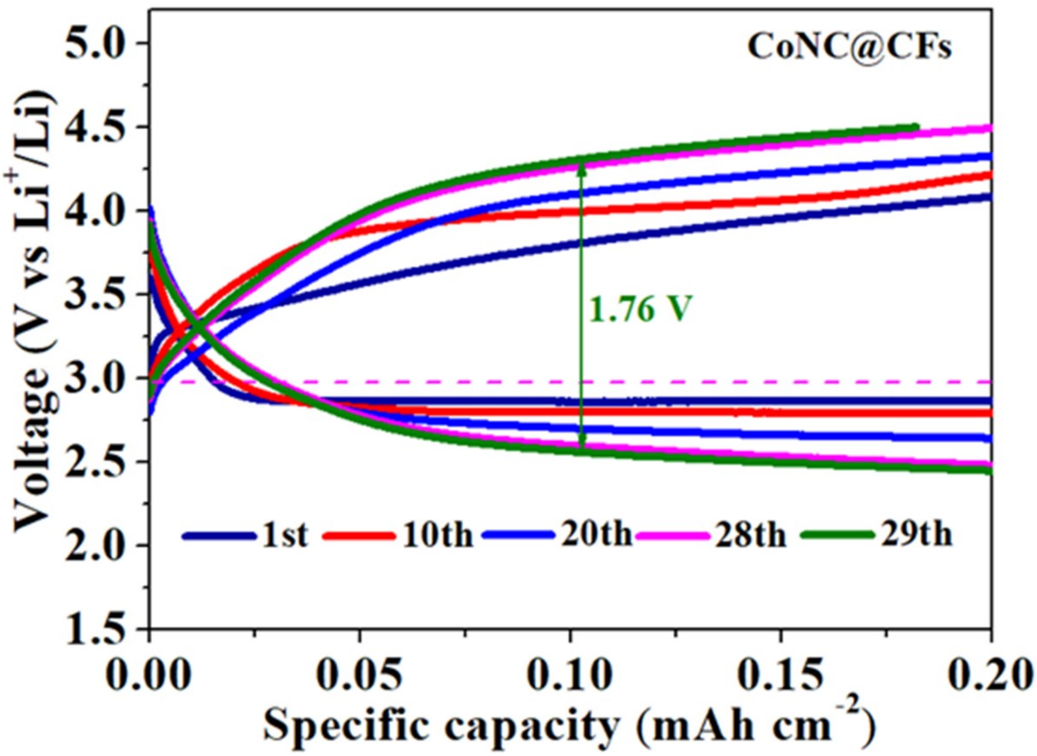

Fig. S10. Cycle performance of CoNC@CNFs electrodes at a current density of 0.02 mA cm^{-2}.

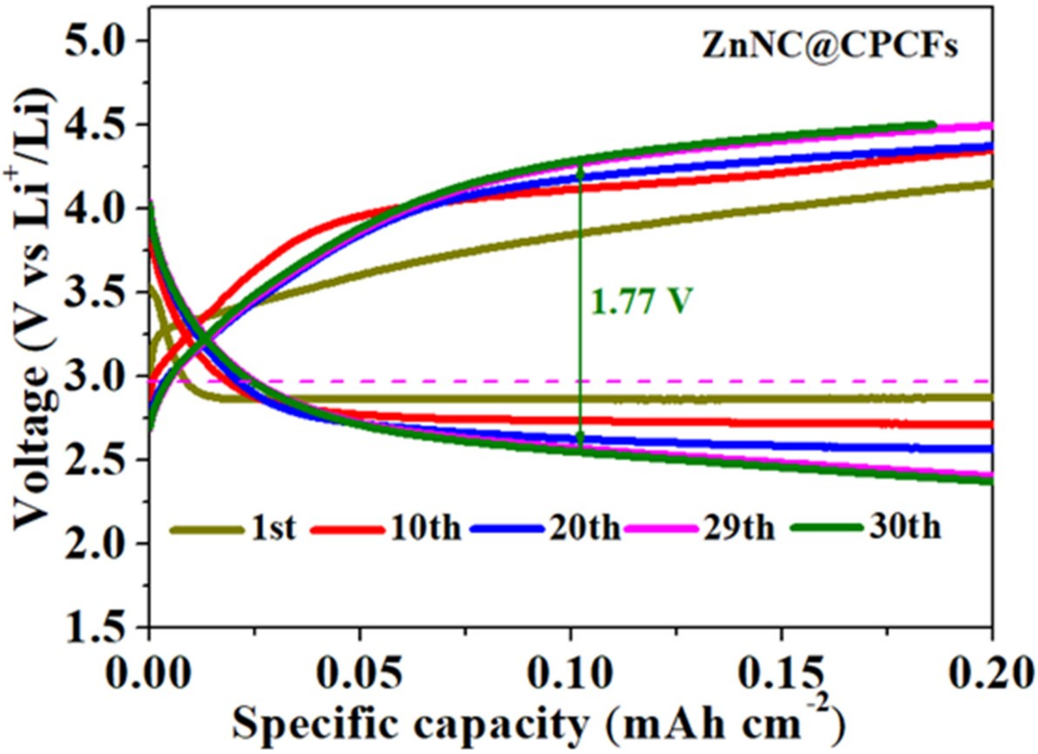

Fig. S11. Cycle performance of ZnNC@CPCNFs electrodes at a current density of 0.02 mA cm^{-2}.

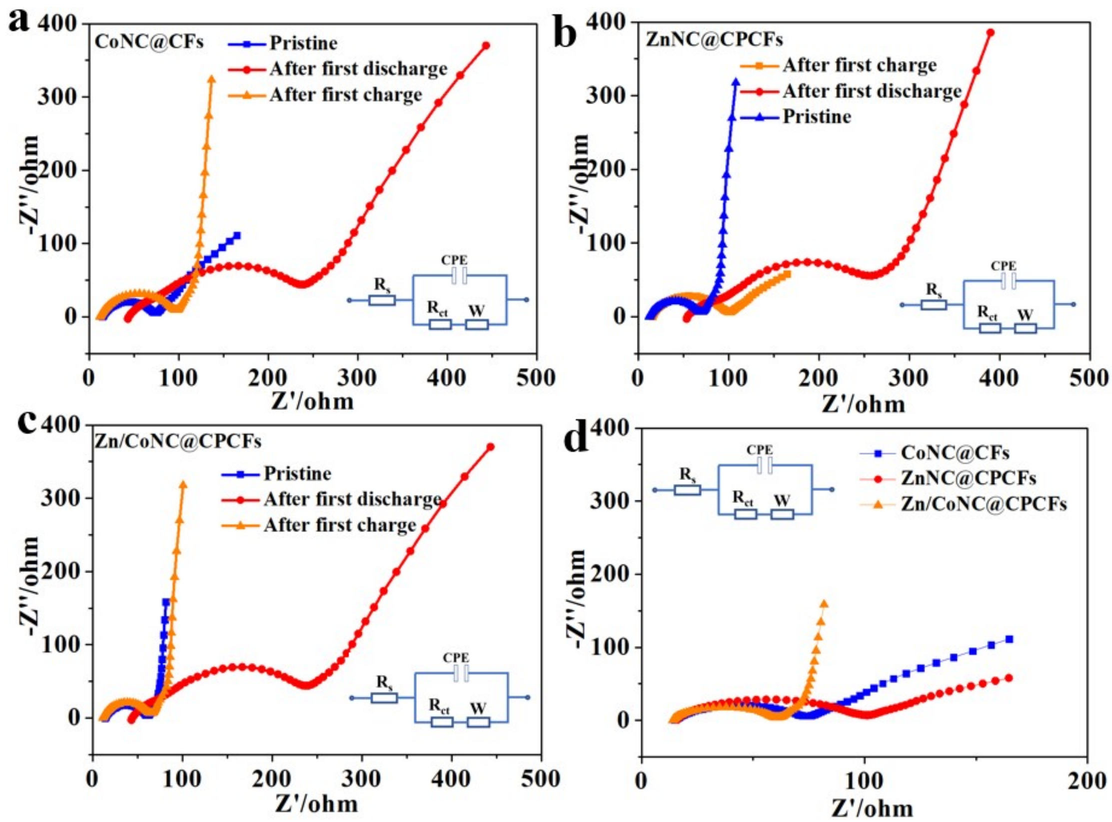

Fig. S12. Nyquist plots of Li-O_2 cells with different fabricated air-cathodes under different cycling conditions of original state, discharge to 6 mAh cm^{-2}, and charge to 6 mAh cm^{-2} (a-c); comparison of the Nyquist plots of three kinds air-cathodes of Li-O_2 cells in the original state (d).

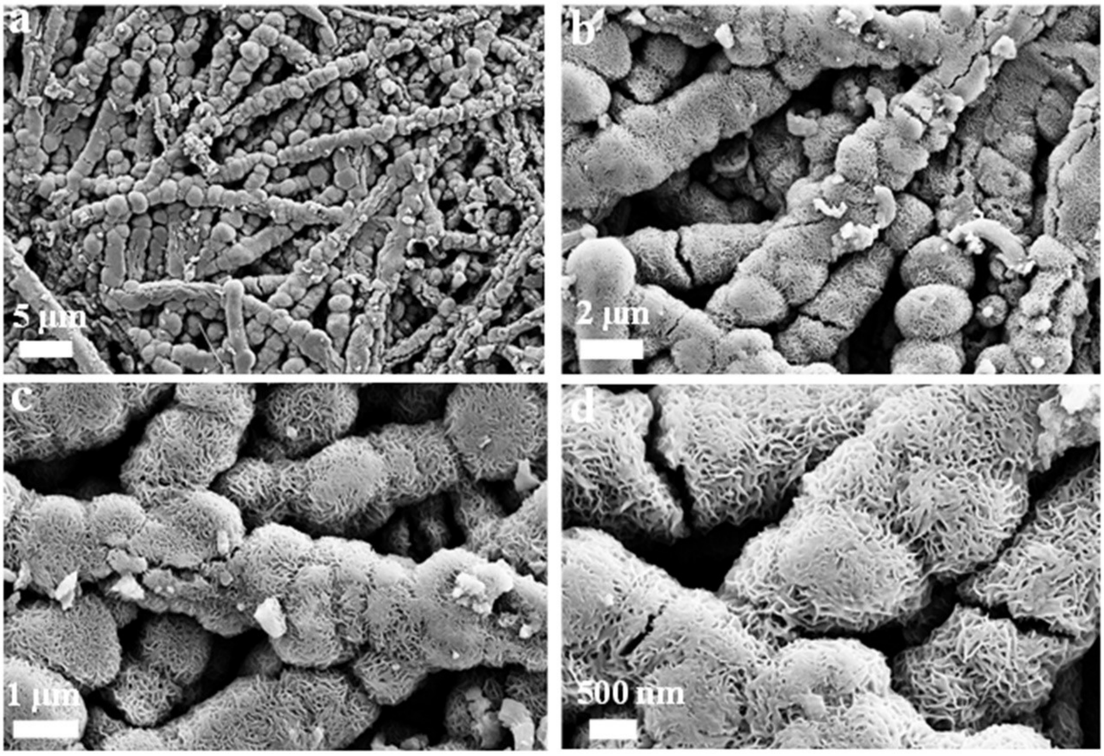

Fig. S13. (a–d) the corresponding SEM images of Zn/CoNC@CPCNFs electrode at a discharge capacity of 6 mAh cm^{-2}.

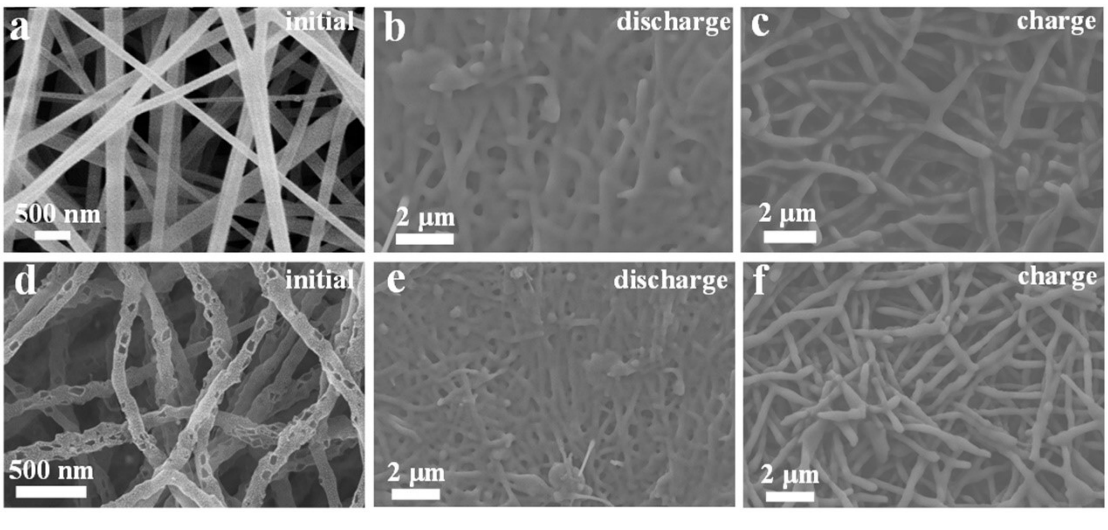

Fig. S14. (a–c) the corresponding SEM images of CoNC@CNFs electrode at different discharge and charge states; (d-f) the corresponding SEM images of ZnNC@CPCNFs electrode at different discharge and charge states.

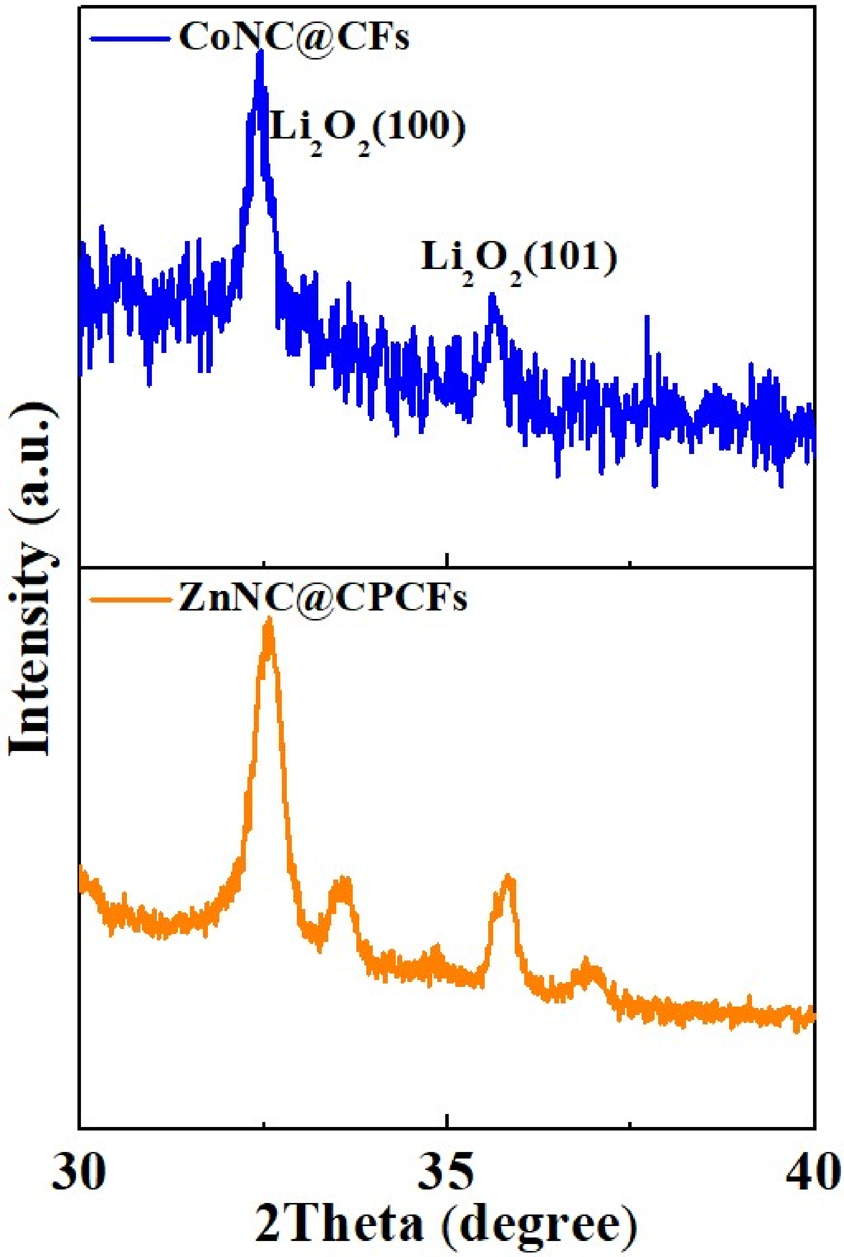

Fig. S15. XRD patterns of ZnNC@CPCFs and CoNC@CFs electrodes upon recharge.

Fig. S16. the value of conductivity of fabricated three electrode. (a) Zn/CoNC@CPCFs; (b) ZnNC@CPCFs; (c) CoNC@CFs.

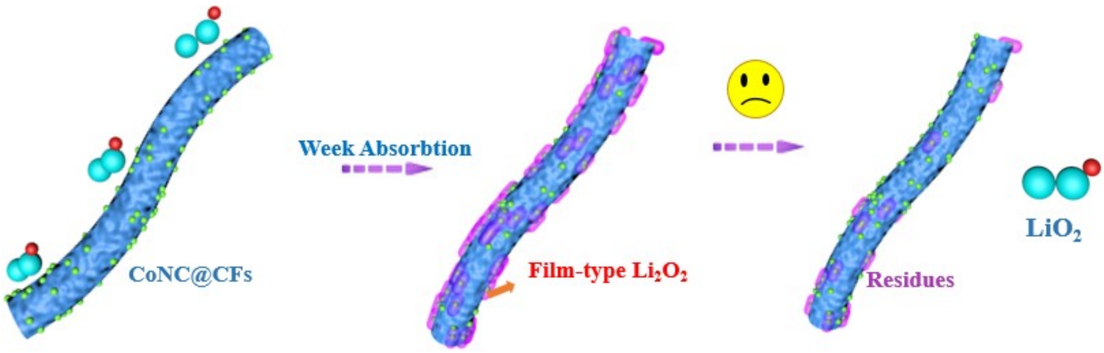

Fig. S17. Schematic diagram of the working mechanism of CoNC@CFs electrodes.

Table S1. The information of BET surface area, total pore volume, pore width of as-prepared three samples.

Samples	S_{BET} (m^2/g)	V_{total} (cm^3/g)	V_{micro} (cm^3/g)	Pore width (nm)	Pore size (nm)
Zn/CoNC@CPCFs	321.78	0.307	0.100	3.825	~2.0, 100
CoNC@CFs	20.90	0.037	0.003	7.088	~2.0, 100
ZnNC@CPCFs	276.85	0.278	0.084	4.022	~2.0, 100

Table S2. The surface atom percentage of Zn/CoNC@CPCFs, ZnNC@CPCFs and CoNC@ CFs.

Samples	Percentage of different elements (%)				
	C	Zn	Co	N	O
Zn/CoNC@CPCFs	69.67	3.55	1.65	8.00	17.43
CoNC@CFs	69.93		10.68	6.81	12.58
ZnNC@CPCFs	77.58	8.99		7.09	6.35

Table S3. ICP-OES results of Zn/CoNC@CPCFs catalysts.

Catalyst	Co (wt%)
Zn/CoNC@CPCFs	1.80

Table S4. The terminal value discharge/charge voltage difference.

Catalyst	terminal value discharge/charge voltage difference (V)			
	0.02 mA cm^{-2}	0.04 mA cm^{-2}	0.08 mA cm^{-2}	0.12 mA cm^{-2}
Zn/CoNC@CPCFs	0.36	0.78	0.99	1.16
ZnNC@CPCFs	1.49	1.73	1.80	1.88
CoNC@CFs	1.40	1.73	1.84	1.92

Table S5. The detailed values of Rct and Rs of the EIS equivalent circuit.

Catalyst	Pristine		After first discharge		After first charge	
	Rct (Ω)	*Rs* (Ω)	*Rct* (Ω)	*Rs* (Ω)	*Rct* (Ω)	*Rs* (Ω)
Zn/CoNC@CPCFs	49.4	12.8	195.7	43.6	51.8	13.4
ZnNC@CPCFs	86.2	15.8	210.2	53.2	85.0	16.5
CoNC@CFs	60.3	14.6	195.7	43.6	83.8	14.0

Table S6. Comparison of various catalysts in their half-recharge overpotential and discharge capacity.

Catalyst	Half-recharge Overpotential	Specific capacity	Current density (mA cm^{-2})	Ref
Zn/CoNC@CPCFs	0.59 V	12451 mAh g^{-1} (12.12 mAh cm^{-2})	0.02	This work
$Ru_{0.3}$ SAs-NC	1.21 V	13424 mAh g^{-1}	0.02	[1]
CMPACs-Fe		7800 mAh g^{-1}	0.02	[2]
C_P	1.44 V	20300 mAh g^{-1}	0.02	[3]
Ru/ITO	0.67 V	2.5 mAh cm^{-2}	0.025	[4]
Ag/β-MnO_2	0.96 V	811 mAh g^{-1}	0.02	[5]
CA	0.78 V	500 mAh g^{-1}	0.02	[6]

Reference

[1] Hu X, Luo G, Zhao Q, et al. Ru single atoms on N-doped carbon by spatial confinement and ionic substitution strategies for high-performance Li−O_2 batteries. J Am Chem Soc., 2020, 142, 16776–16786.

[2] Li D, Wang Q, Yao Y, et al. New Application of Waste Citrus Maxima Peel-Derived Carbon as an Oxygen Electrode Material for Lithium Oxygen Batteries. ACS Appl Mater Interfaces, 2018, 10, 32058–32066.

[3] Zhao T, Yao Y, Yuan Y, et al. A universal method to fabricating porous carbon for Li-O_2 battery. Nano Energy, 2021, 82, 105782.

[4] Li F, Tang DM, Chen Y, et al. Ru/ITO: A carbon-free cathode for nonaqueous Li-O_2 battery. Nano Lett., 2013, 13, 4702–4707.

[5] Huang Z, Zhang M, Cheng J, et al. Silver decorated beta-manganese oxide nanorods as an effective cathode electrocatalyst for rechargeable lithium-oxygen battery. J Alloys Compd., 2015, 626, 173–179.

[6] Li S, Wang M, Yao Y, et al. Effect of the Activation Process on the Microstructure and Electrochemical Properties of N-Doped Carbon Cathodes in Li-O2 Batteries. ACS Appl Mater Interfaces, 2019, 11, 34997–35004.